Design Concerns for In-body Antennas Based on Frequency Analysis of Fundamental Radiation Limitations

Zvonimir Sipus, Marko Bosiljevac, Denys Nikolayev, Anja Skrivervik

Design Concerns for In-body Antennas Based on Frequency Analysis of Fundamental Radiation Limitations

Zvonimir Sipus[1], Marko Bosiljevac[1], Denys Nikolayev[2], Anja Skrivervik[2]
[1] University of Zagreb Faculty of Electrical Engineering and Computing, Zagreb, Croatia
zvonimir.sipus@fer.hr, marko.bosiljevac@fer.hr
[2] Microwave and Antenna Group (MAG), Ecole Polytechnique Fédérale de Lausanne, Switzerland
denys.nikolayev@epfl.ch, anja.skrivervik@epfl.ch

***Abstract*—Fundamental radiation limitations of in-body or implantable antennas should give us an estimate on the feasibility of some desired system. It was shown that near-field effects and distance to the body - freespace boundary are critical aspects, while the shape doesn't play a major role in the achievable power. Through the frequency analysis of these limitations in this paper we provide another perspective and show how rigorous and approximate approach to near-field and reflection losses manifest in the results. This is demonstrated on a spherical body example which contains a small spherical implant which can be placed at different positions within the body in order to simulate different implant depths. The results reveal that reasonably accurate description of in-body loss mechanisms can be achieved using our previously defined fundamental radiation limitations for power density, however, depending on the frequency different loss aspects must be treated with special care.**

***Index Terms*—in-body antennas, radiation limitation, spherical-mode analysis.**

I. Introduction

Recent advances in electronics and wireless possibilities have inspired a large growth of interconnected sensors and devices which are dedicated to improving health care for various types of patients. Design of such medical implants is quite a challenge for engineers due to numerous restrictions in terms of size, allowed materials, required longevity and similar. Also, from the perspective of communication link and antenna design the small size and losses of the body tissue result in a very complex design situation.

In order to estimate the possibilities of a certain design it is beneficial to understand the limits in the performance of small antennas placed in body environment. Many studies exist where limits of the performances of electrically small antennas have been studied (pioneering work started by Chu [1], Wheeler [2], Harrington [3], and continued by Collin et al. [4], Fante [5] and Fano [6]). Also, further advances in this topic have been demonstrated in [7-10]. These principles, however, are valid for antennas in free space environment, while the implanted scenario places the antenna into a very lossy medium. Commonly used practices cannot be applied in these scenarios and alternative strategies need to be defined. In [11] it was shown that fundamental antenna characteristics like the far field, the antenna radiation pattern or the bandwidth do not apply when the antenna radiates into an infinite lossy medium.

This inspires us to investigate theoretical and practical limits of antennas when radiating into a lossy medium. Recent advances in characterization and in-body link modelling can be found in [12-13] however, our aim is to use canonical models (spherical and cylindrical phantoms) to investigate fundamental physical limits on the total power and maximal power density that can reach free space for a specific implanted antenna scenario. This gives a rough estimate of the realistic scenario but provides useful insights into the fundamental radiation limitations. [14, 15].

II. Model and Analysis Method

The basis of our analysis is a spherical model of a human body which is a rough estimate, but it gives valuable insight [16] into the investigated topic. Fig. 1 presents the analyzed structure and its geometry. The outer sphere represents the body tissue (with radius r_{body}) and the smaller sphere is the encapsulation of the implanted antenna.

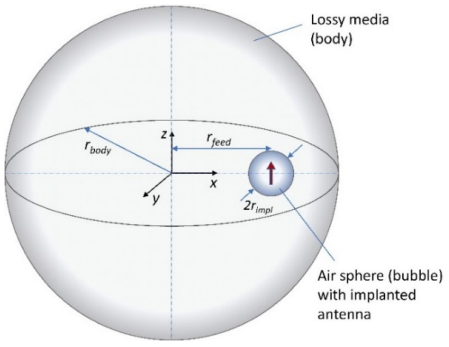

Fig 1. View of the analyzed structure with the excitation moved away from the center.

The sphere modeling the body can be either homogeneous or formed by concentric layers in order to mimic a part of the human body (skin, fat, muscle, etc.) by using dielectric properties that are similar to those of real human tissues. The implanted antenna is modeled as either an electric or a magnetic dipole encapsulated in a small sphere with radius r_{impl} filled with air.

In order to optimize the speed and optimization, our numerical procedure is based on spherical-wave modal expansion. The electromagnetic field in a spherical structure (with zero free-charge density) can be represented using vector spherical harmonics [17], [18] as:

$$\mathbf{E} = -\sum_{n}\sum_{m} a_{mn}\mathbf{M}_{mn} + b_{mn}\mathbf{N}_{mn}\,, \tag{1}$$

where

$$\mathbf{M}_{mn} = \nabla\times\hat{\mathbf{r}}\psi_{mn}\,, \qquad \mathbf{N}_{mn} = \frac{1}{k}\nabla\times\mathbf{M}_{mn} \tag{2}$$

$$\psi_{mn} = \frac{1}{\beta r}\hat{Z}_n(\beta r)P_n^m(\cos\theta)e^{jm\phi} \tag{3}$$

Here ψ_{mn} is the elementary solution of the Helmholtz differential equation, i.e. $\hat{Z}_n$ denotes Schelkunoff type of spherical Bessel or Hankel functions [18], β denotes the wavenumber of the considered media and $\hat{\mathbf{r}}$ is the unit vector in r-direction.

As it can be seen in Fig. 1 the structure of interest consists of two spherical structures - the spherical model of a body and the spherical model of an implanted antenna. Each spherical structure can be multilayered and can be separately analyzed using the spherical-wave modal expansion approach described with eqs. (1)–(3). Therefore, the main challenge in the analysis of the structure in Fig. 1 lies in connecting two spherical problems that have displaced centers of coordinate systems. Details of this procedure are given in [14-15].

III. RESULTS

A. Initial observations

The scenario shown in Fig. 1. is simulated using our code and CST Microwave Studio for an antenna implanted in two different phantoms: a spherical phantom and a cubic body phantom where the cube side length is equal to the diameter of the considered sphere. The working frequency is 403.5 MHz, the body sphere has r_{body} = 9 cm radius and permittivity is ε_{body} = 43.50 – j34.75 [19, IEEE Head model]. The implanted antenna in this case is a short electrical dipole located in a 2mm diameter air sphere (implanted antenna) placed in the center of the body phantom. The power density (real part) is observed on the line passing through the center of the cube side and perpendicular to the excitation electric dipole) and it is given in Fig. 2. This result indicates that the actual shape of the body is not crucial. Moreover, this result validates the applicability of the spherical model in our investigation since all the results agree very well. Note that the power density is normalized with the factor $W_0/(8\pi/3)\cdot(r_{obs}-r_{feed})^2$, where W_0 is the maximum value of the real part of the power density component normal to the surface of implanted antenna, i.e., just inside the lossy medium.

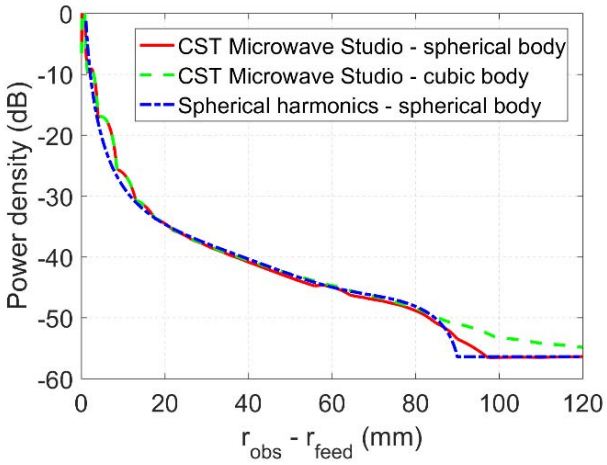

Fig. 2. Radial component of real part of the normalized power density at different distances from the implanted antenna placed in spherical and cubic body. The source is placed at the center of the body.

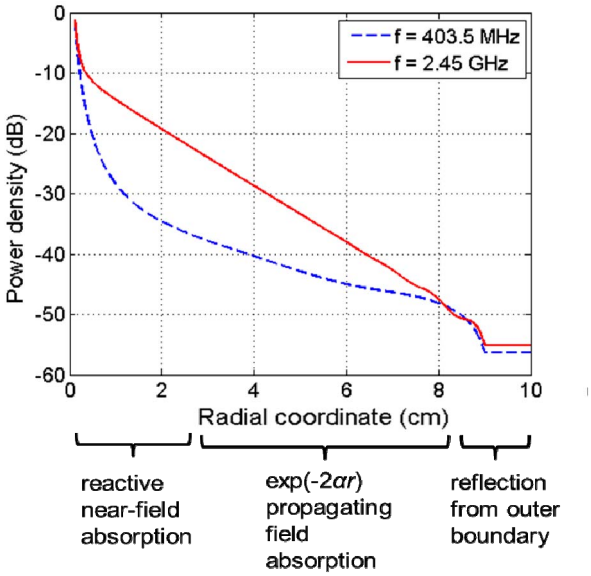

Fig. 3. Radial component of real part of the normalized power density at different distances from the implanted antenna. The source is in the center of 9 cm spherical phantom.

The results in Fig. 2. show three regions crucial for understanding the propagation mechanism through the body when the source is implanted. This is further highlighted in Fig. 3. where the radial component of real part of the normalized power density is observed for two common

frequencies, 403.5 MHz (as in the first case) and 2.45 GHz ($\varepsilon_{r,body}$ = 39.2 - j13.2 at 2.45 GHz). Three regions are highlighted (near-field absorption, propagating field absorption, reflection from the boundary) and although there is a large difference in frequencies, in this particular case the final power density reaching free space is comparable. This led us to use the developed expressions for the available power reaching free space [20] and investigate what is the frequency behaviour of the available power.

A similar investigation was performed for a particular case in [21], however we wanted to expand on this by studying how the expressions for fundamental limits behave for different frequencies. These expressions were derived in [20], and here only the final results are repeated for convenience for the case of the dominant spherical mode due to an electric dipole excitation (the mode that is least attenuated in the lossy media; the Hankel functions and their derivatives are replaced with the analytic expressions);

The reactive near-field the losses and corresponding efficiency e can be expressed with

$$e_{\substack{\text{losses}\\ \text{in the}\\ \text{reactive}\\ \text{near-field}}} = \frac{\left|\bar{\beta}\right|^2 \mathrm{Re}\{\bar{\eta}\}}{\mathrm{Re}\left\{\bar{\eta}\cdot\left(\left|\bar{\beta}\right|^2 + \frac{2\alpha}{r} + \left(1-\frac{\bar{\beta}^*}{\bar{\beta}}\right)\frac{1}{r^2} - j\frac{1}{\bar{\beta}r^3}\right)\right\}} \tag{4}$$

This expression can be approximated for the dominant term as

$$e_{\substack{\text{losses}\\ \text{in the}\\ \text{reactive}\\ \text{near-field}}} = \frac{\left|\bar{\beta}\right|^2 \mathrm{Re}\{\bar{\eta}\}}{\mathrm{Im}\left\{\bar{\eta}/\left(\bar{\beta}r_{impl}^3\right)\right\}} \,. \tag{5}$$

The propagating field absorption efficiency is equal

$$e_{\substack{\text{propagating}\\ \text{field}\\ \text{absorption}\\ \text{losses}}} = \exp(-2\alpha(r_{body} - r_{impl})) \tag{6}$$

and the efficiency due to reflections at the outer boundary

$$e_{\substack{\text{losses}\\ \text{due to}\\ \text{reflections}}} = \frac{\mathrm{Re}\left\{|T|^2/Z_{air}\right\}}{\mathrm{Re}\left\{1/Z_{body}\right\}}, \qquad T = \frac{2Z_{air}}{Z_{air}+Z_{body}} \,. \tag{7}$$

The spherical characteristic impedances Z_{air} and Z_{body} for the dominant spherical mode are equal to

$$Z^J(\beta r) = \frac{E_\theta}{H_\phi} = -\frac{E_\phi}{H_\theta} = \eta\frac{e^{-j\beta r} - je^{-j\beta r}/\beta r - e^{-j\beta r}/(\beta r)^2}{e^{-j\beta r} - je^{-j\beta r}/\beta r} \tag{8}$$

The reflection losses can be well approximated using large-radius variation resulting in:

$$e_{\substack{\text{losses}\\ \text{due to}\\ \text{reflections}}} \approx \left|\frac{2\sqrt{\varepsilon_{body}}}{1+\sqrt{\varepsilon_{body}}}\right|^2 \Big/ \mathrm{Re}\left\{\sqrt{\varepsilon_{body}}\right\}. \tag{9}$$

With these expressions it is possible to express the power density reaching free-space as

$$W_{\substack{\text{reaching}\\ \text{free}\\ \text{space}}} = W_{\substack{\text{entering}\\ \text{the}\\ \text{body}}} \cdot e_{\substack{\text{losses}\\ \text{in the}\\ \text{reactive}\\ \text{near-field}}} \cdot e_{\substack{\text{propagating}\\ \text{field}\\ \text{absorption}\\ \text{losses}}} \cdot e_{\substack{\text{losses}\\ \text{due to}\\ \text{reflections}}} \tag{10}$$

B. Frequency analysis

In order to compare the results with existing work the focus will be on the 10 cm radius sphere which was used in [21]. In order to discuss the formula for power density reaching free space a single-layer muscle structure was considered. The frequency variation of complex permittivity is given in [22], and the radius of the centrally positioned implanted antenna is 5 mm.

Fig. 4. shows the frequency dependence of the power density reaching the free-space for several different ways of calculating the power density. Indicated as "Power density" in the figures is the power density calculated completely rigorously using the spherical harmonics code, while other curves are plotted using expressions (4) – (10) with different ways of calculating the reflection losses. From Fig. 4 it is clear that the fundamental limit gives the estimation of the maximum power density at the body surface. Note that in the expression for the fundamental limit there are no reflection losses since it is hard to predict the minimum reflection losses [20]. For lower frequencies the reflections are larger since the EM field just outside the body is in the reactive near-field which increases the magnitude of the reflection coefficient. Therefore, for a symmetric case, i.e. for the implantable antenna in the center of the body, one should use the rigorous expression for the efficiency due to reflections (eq. (7)).

In the presented results in Fig. 4.a there is a non-physical increase of the power density around 1 GHz, i.e. around frequencies for which the reactive near-field efficiency approaches one. For such frequencies we cannot just use the dominant-term expression (given with eq. (5)), i.e. we should use the more complicate rigorous expression given with eq. (4). The results obtained with the rigorous expression are given in Fig. 4.b, and an excellent prediction of the power density just outside the body is obtained. The same type of results is achieved for a dual case – magnetic (see Fig.5). Note that there is a large difference in obtainable power density just outside the body for lower frequencies since the reactive near-field is present in a large part of the body and the losses in reactive near-field zone are much smaller for a magnetic dipole based implantable antenna. The magnetic dipole excites much stronger magnetic fields in the vicinity of the dipole, which do not dissipate in the body since there are no magnetic losses present in human tissues.

For non-symmetric case, i.e. for an implantable antenna with off-center position, for the estimation of the reflection losses one should use the approximate expression for the efficiency due to reflections given with eq. (9). The reason why one needs to use the expression that is based on large-radius approximation is based on the fact that the spherical symmetry is violated and consequently each spherical wave excited by the source is scattered from the outer boundary as a spectrum of spherical waves of different order. The results for both electric and magnetic dipole excitations are given in Fig. 6. Again, a good prediction of the power density just outside the body is obtained.

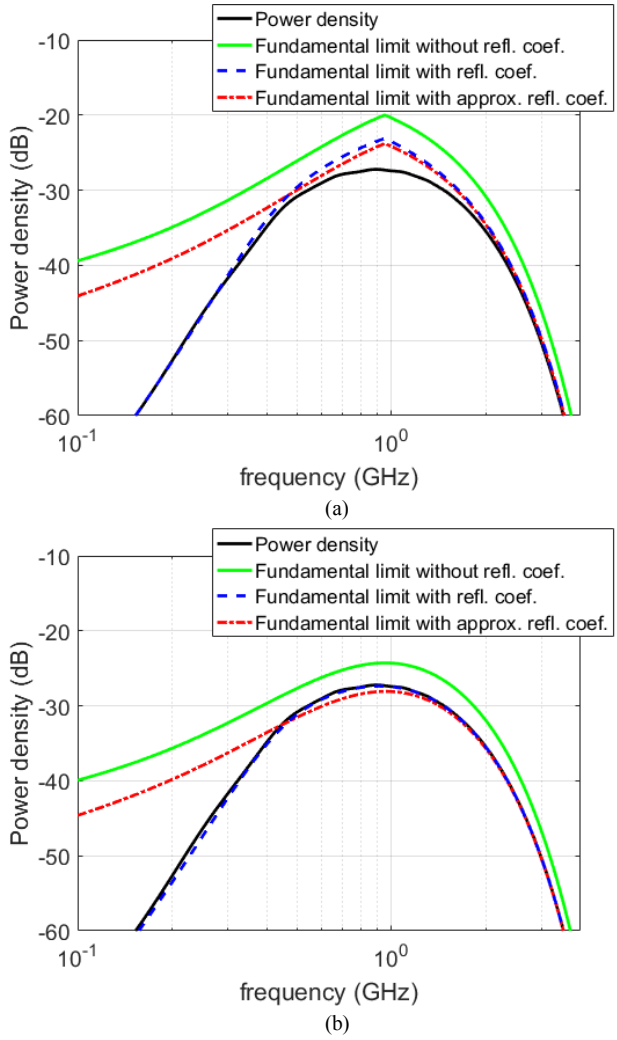

Fig. 4. Radial component of real part of the normalized power density as a function of frequency for electric dipole excitation; (a) approximate near-field expression, (b) rigorous near-field expression.

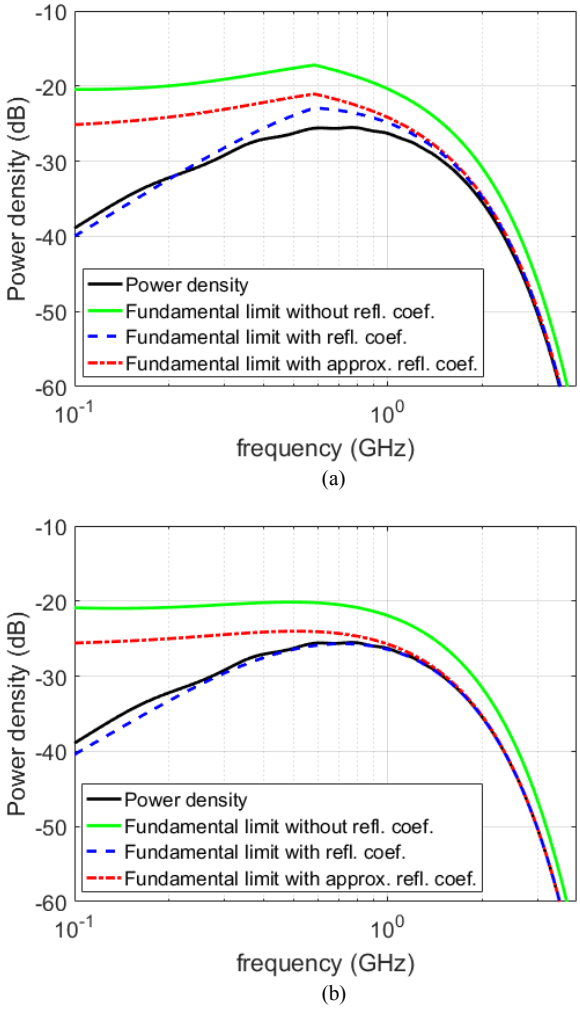

Fig. 5. Radial component of real part of the normalized power density as a function of frequency for magnetic dipole excitation; (a) approximate near-field expression, (b) rigorous near-field expression.

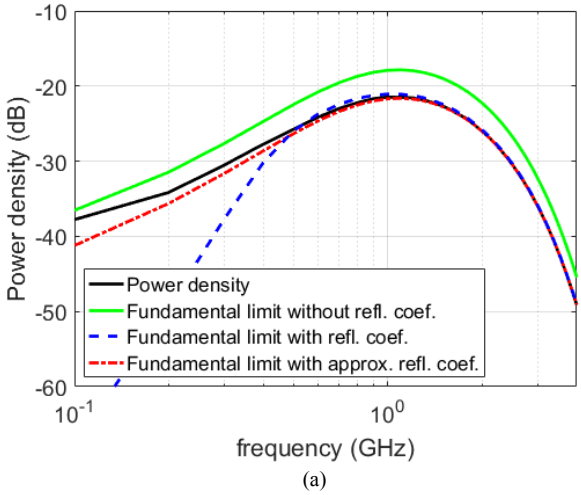

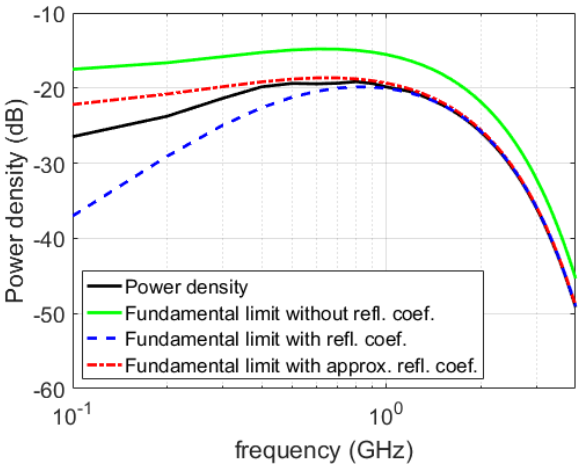

(b)

Fig. 6. Radial component of real part of the normalized power density as a function of frequency calculated using rigorous near-field expressions for the source moved 3 cm away from the center; (a) electric dipole case, (b) magnetic dipole case.

IV. Conclusion

Fundamental radiation limitations for small implanted antennas are largely undefined. Using a spherical body model as a starting point we previously demonstrated that limits on the available power density can be determined. In this paper we expanded the investigation and analyzed the frequency dependence of these limits and placed them in perspective with the loss mechanisms present in the body. The analysis of the results revealed different perspectives for handling near-field losses and reflection losses. In cases with spherical symmetry approximating the near-field losses with only the dominant term leads to errors in the prediction of the power density and needs to be corrected by using a more rigorous expression. This is also valid when considering reflection losses i.e. the rigorous formulation needs to be considered. However, when there is no spherical symmetry, i.e. the source is not in the center of the sphere, the large radius approximation for reflection losses provides much better results. These findings indicate that the developed limits have to be observed also in context of frequency and position in order to provide good initial approximations for the design of implanted systems.

Acknowledgment

This research has been supported in part by the European Regional Development Fund under the grant KK.01.1.1.01.0009 (DATACROSS).

References

[1] L.J. Chu, "Physical limitations on omni-directional antennas", *Journal of Applied Physics*,. 19, 1948, pp. 1163-1175.

[2] H.A. Wheeler, "Fundamental Limitations of Small Antennas", *Proc. of the IRE*, 1947, pp. 1479-1484.

[3] R.F. Harrington, "On the Gain and Beamwidth of Directional Antennas", *IRE Transactions on Antennas and Propagation*, vol. AP-6, 1958, pp. 219-225.

[4] R.E Collin and S. Rothschild, "Evaluation of Antenna Q", *IEEE Transactions on Antennas and Propagation*, vol. AP-12, 1964, pp. 23-27.

[5] R.L. Fante, "Quality factor of general ideal antennas", *IEEE Transactions on Antennas and Propagation*, vol. AP-17, 1969, pp. 151-155.

[6] Fano, R. M., "Theoretical limitations on the broadband matching of arbitrary impedances", *J. Franklin Inst.* 249, 57–83 see also 139–154, 1950.

[7] A.D. Yaghjian and S.T. Best, "Impedance, Bandwidth and Q of Antennas", *IEEE Transactions on Antennas and Propagation*, vol. AP-53, 2005, pp. 1298-1324.

[8] R.C. Hansen, Electrically small, Superdirective and Superconductive Antennas, John Wiley and sons, New Jersey, 2006.

[9] S.R. Best and A.D. Yaghjian, "The Lower Bound on Q for Lossy Electric and Magnetic Dipole Antennas", *IEEE Antennas and Wireless Propagation Letters*, vol. 3, 2004, pp. 314-316.

[10] M Gustafsson, C. Sohl and G. Kristensson, "Physical limitations on antennas of arbitrary shape", *Proc. R. Soc. A*, vol. 463, pp. 2589-2607, 2007.

[11] R. Moore, "Effects of a surrounding conducting medium on antenna analysis," *IEEE Transactions on Antennas and Propagation*, vol. AP-11, no. 3, pp. 216–225, May 1963.

[12] C. Ehrenborg and M. Gustafsson, "Calculating physical bounds for in-body antennas", Proc. the 12th European Conference on Antennas and Propagation, EuCAP 2018, London, UK, pp 1-3.

[13] J. Faerber et al., "In vivo characterization of wireless telemetry module for a capsule endoscopy system utilizing a conformal antenna," *IEEE Transaction on Biomedical Circuits and Systems*, vol. 12, pp. 95-104, Feb. 2018.

[14] M. Bosiljevac, Z. Sipus, A.K. Skrivervik, "Propagation in Finite Lossy Media: an Application to WBAN", *IEEE Antennas and Wireless Propagation Letters*, vol.14, pp. 1546 - 1549, 2015.

[15] M. Bosiljevac, Benjamin Fuchs, A.K. Skrivervik and Z. Sipus, "Study of wearable WBAN antenna properties based on spherical body model", Proc. the 10th European Conference on Antennas and Propagation, EuCAP 2013, Davos, Switzerland, pp 1-3.

[16] J. Kim and Y. Rahmat-Samii, "Implanted antenna inside a human body: simulations, design, and characterization," *IEEE Transactions on Antennas and Propagation*, vol. AP-52, 2004, pp. 1934-1943.

[17] J. A. Stratton, *Electromagnetic theory*, McGraw-Hill N.Y.,1941.

[18] R. F. *Harrington*, *Time Harmonic Electromagnetic Fields*, McGraw-Hill, New York, 1961.

[19] Evaluating Compliance With FCC Guidelines for Human Exposure to Radiofrequency Electromagnetic Fields, 97–01 ed. Washington, DC: Federal Communication Commission (FCC) Std. Supplement C, OET Bulletin 65, p. 35, 2001.

[20] A. Skrivervik, M. Bosiljevac, Z. Šipuš, "Fundamental Limits for Implanted Antennas: Maximum Power Density Reaching Free Space", *IEEE Transactions on Antennas and Propagation*, Vol. 67 , No. 8, pp. 4978-4988, 2019.

[21] D. Nikolayev, W. Joseph, M. Zhadobov, R. Sauleau, and L. Martens, "Optimal Radiation of Body-Implanted Capsules," Physical Review Letters, Vol. 122, 108101, 2019.

[22] S. Gabriel, R.W. Lau, and C. Gabriel, "The dielectric properties of biological tissues: III. Parametric models for the dielectric spectrum of tissues," Phys. Med. Biol., vol. 41, 2271, 1996.